HHS Public Access

Author manuscript

Magn Reson Med. Author manuscript; available in PMC 2018 February 01.

Published in final edited form as:

Magn Reson Med. 2017 February ; 77(2): 826–832. doi:10.1002/mrm.26123.

Development of a Symmetric EPI Framework for Clinical Translation of Rapid Dynamic Hyperpolarized ^{13}C Imaging

Jeremy W. Gordon[1], **Daniel B. Vigneron**[1], and **Peder E.Z. Larson**[1]

[1]Department of Radiology & Biomedical Imaging, University of California-San Francisco

Abstract

Purpose—To develop symmetric echo-planar imaging (EPI) and a reference scan framework for hyperpolarized ^{13}C metabolic imaging.

Methods—Symmetric, ramp-sampled EPI with partial Fourier reconstruction was implemented on a 3T scanner. The framework for acquiring a reference scan on the ^{1}H channel and applied to ^{13}C data was described and validated in both phantoms and *in vivo* metabolism of [1-^{13}C]pyruvate.

Results—Ramp-sampled, symmetric EPI provided a substantial increase in the SNR of the phantom experiments. The reference scan acquired on the ^{1}H channel yielded ^{13}C phantom images that varied in mean signal intensity <2%, as compared to ^{13}C images reconstructed with a reference scan directly measured on the ^{13}C channel. The structural similarity index and dynamic time course from *in vivo* ^{13}C data further support the application of a ^{1}H reference scan to ^{13}C data to mitigate Nyquist ghost artifacts.

Conclusion—Ramp-sampled, symmetric EPI with spectral-spatial excitation of a single metabolite provides a fast, robust and clinically efficacious approach to acquire hyperpolarized ^{13}C dynamic molecular imaging data. The gains of this efficient sampling, combined with partial Fourier methods, enables large matrix sizes required for human studies.

Introduction

Advances in hyperpolarization (HP) have enabled real-time molecular imaging that was heretofore impossible with magnetic resonance (1). Using the dynamic nuclear polarization (DNP) technique, spins are exogenously polarized to four orders of magnitude greater than Boltzmann equilibrium. Metabolically active substrates, such as [1-^{13}C]pyruvate (2), are transported into cells and undergo enzymatic conversion into downstream metabolites on the timescale of an HP experiment (~1-2 minutes). This technique is being translated into the clinic, primarily for cancer and cardiac metabolism studies. A Phase 1 clinical trial demonstrated both safety and the feasibility of hyperpolarized [1-^{13}C]pyruvateMR with up-regulated conversion to [1-^{13}C]lactate conversion observed in biopsy-proven prostate cancer patients (3).

Corresponding Author: Jeremy Gordon, 1700 4th St., Byers Hall 102, San Francisco, CA 94158.

This first clinical trial used a ^{13}C spectroscopic data acquisition method, which even with an echo-planar spectroscopic readout, required an acquisition time of 8-12 seconds for 3D volumetric coverage of the prostate with a spatial resolution of $0.34cm^3$.This spectroscopic data demonstrated increased HP [1-^{13}C]lactate to [1-^{13}C]pyruvate ratios in the prostate cancer patients, but the acquisition method had the drawbacks of relatively long temporal resolution, preventing accurate dynamic measurements of metabolism, and the complex EPSI reconstruction was performed offline, not on the clinical scanner.A different approach for rapid volumetric HP ^{13}C MRI acquisition is selective excitation of a single resonance followed by a single shot flyback EPI readout (4). This technique was developed and applied to study the dynamics of [1-^{13}C]lactate in preclinical cancer models following injection of [1-^{13}C]pyruvate with a 3.5s temporal resolution over a 100s time window (4). Although this study showed significant differences in [1-^{13}C]lactate dynamics between early and late stage transgenic prostate cancers, without the detection of [1-^{13}C]pyruvate signals the measurement of conversion rates could not be made. Utilizing the chemical shift differences between the lactate and pyruvate resonances, acquisitions of both compounds can be acquired simultaneously (5), but suffer from FOV restrictions and sub-optimal SNR.

A major challenge facing these HP acquisition techniques is the limited imaging window, an outcome of the inexorable decay to the Boltzmann (or thermal) equilibrium polarization. Rapid and RF efficient imaging sequences are therefore of paramount importance to maximize the signal-to-noise ratio (SNR) and resolution in ^{13}C experiments. Using a singleband spectral-spatial RF pulse (4,6), individual metabolites can be excited and rapidly imaged with a single excitation. Due to the slow transverse decay of ^{13}C-labeled metabolites (7), a low bandwidth/long duration readout can be used to maximize SNR efficiency. An echo-planar imaging (EPI) readout trajectory in particular is well-suited for hyperpolarized imaging because of its rapid, efficient sampling and relative robustness to off-resonance artifacts. Flyback EPI trajectories have been used (5,8) for rapid metabolic imaging due to their insensitivity to timing delays and ease of implementation, but this approach suffers from a reduced SNR efficiency because of the lack of encoding during the flyback gradient. The lower ^{13}C gyromagnetic ratio also results in reduced scan efficiency and longer echo times (TE) that exacerbate EPI-related image artifacts. Translating this technique to clinical ^{13}C imaging requires further improvements in scan efficiency in order to improve SNR and enable rapid and robust metabolic imaging *in vivo*.

Symmetric EPI is an appealing alternative to flyback EPI. By encoding k-space on both the positive and negative gradient lobes, the echo-spacing can be substantially reduced, resulting in improved SNR and less sensitivity to off-resonance. The SNR efficiency is also increased with symmetric EPI due to a higher sampling duty-cycle, and can be further increased by using ramp-sampling. The downside of this approach is that symmetric EPI is prone to Nyquist ghosting artifacts because of delays and inconsistencies between even and odd lines of k-space, which primarily arise from eddy currents and concomitant magnetic fields (9). These errors manifest as an offset between even and odd lines of k-space, resulting in misalignment between the even and odd echoes and resulting in image ghosts that are shifted by half the FOV if left uncorrected (10). These timing delays and inconsistencies can be estimated with a reference scan (11,12), and, by applying a line-by-line phase correction in x-k_y space, Nyquist ghost artifacts can be minimized. However, a reference scan will be

difficult to directly acquire from the hyperpolarized substrate due to the transient magnetization and the narrow window in which to image metabolism.

The goal of this project was to develop and test a new specialized HP ^{13}C EPI acquisition approach with high SNR efficiency and temporal resolution that could be readily translated into future human studies. To that end, we developed and implemented a symmetric, ramp-sampled, partial Fourier EPI sequence for efficient HP ^{13}C imaging. We also developed a framework for acquiring a reference scan from ^{1}H data for application to hyperpolarized ^{13}C data on a clinical 3T MR scanner. Our approach was designed to be robust and SNR-efficient, have reduced EPI off-resonance artifacts, and to eliminate EPI ghosting artifacts, making it well-suited for clinical metabolic imaging studies with hyperpolarized ^{13}C agents.

Methods

All experiments were performed on a clinical 3T scanner (MR 750, GE Healthcare, WI) with a maximum gradient strength of 5 G/cm and a maximum slew-rate of 20 G/cm/ms. A ramp-sampled, symmetric EPI readout with singleband spectral-spatial (SPSP) excitation and partial Fourier reconstruction was developed for use on the clinical GE platform. A reference scan, acquired prior to imaging by disabling the phase-encoding gradients, was used to correct for phase errors that lead to Nyquist ghosts. As the sequence was built off of a product GE sequence, it leveraged the ability to use the reference scan for online reconstruction of ^{13}C metabolite maps, and retained all of the requisite safety and performance features.

A custom built dual-tune ^{1}H/^{13}C volume coil (13) was used for both the thermal phantom and hyperpolarized ^{13}C experiments. For *in vivo* experiments, an enriched 8M ^{13}C urea phantom was used for center frequency and B_1 calibration. The SPSP RF pulse used in all of the EPI acquisitions was designed to excite [1-^{13}C]pyruvate and metabolites at 3T, with a passband FWHM of 120Hz and a stopband of 600Hz. The RF pulse was designed in Matlab (R2014b) using the SPSP RF pulse design toolbox (14). Further information and downloads can be found at http://rsl.stanford.edu/research/software.html or https://github.com/agentmess/hyperpolarized-mri-toolbox.

The SNR efficiency is a function of the duty cycle and k-space trajectory, and will increase from a flyback to a symmetric EPI readout. This gain in SNR efficiency, which is equivalent to the product of the duty cycle and trajectory efficiency, can be defined as (15,16):

$$SNR_{eff,duty} = \sqrt{\frac{T_{readout}}{T_{gradient}}} \quad [1]$$

$$SNR_{eff,uniformity} = \frac{A_k}{\sqrt{\int_k D\left(\vec{k}\right) d\vec{k} \int_k \frac{1}{D\left(\vec{k}\right)} d\vec{k}}} \quad [2]$$

For flyback EPI, $T_{gradient}$ is the duration of the trapezoidal readout gradient plus the flyback gradient. For symmetric EPI, $T_{gradient}$ is the duration of the trapezoidal readout gradient. $T_{readout}$ is the time the analog-to-digital converter is acquiring data. For non ramp-sampled EPI, $T_{readout}$ is equal to the plateau of the readout gradient, while for ramp-sampled EPI, $T_{readout}$ is equal to $T_{gradient}$ minus the duration of the phase encode blip. A_k is the area of the sampled k-space, and D_k is the local k-space sampling density. For partial Fourier, the theoretical SNR efficiency is reduced by 1.15 to account for the reduction in acquisition time for 75% k-space coverage. To quantify the SNR advantages of symmetric EPI, a ^{13}C enriched phantom was used (44mm outer diameter (OD)), consisting of four cylindrical tubes with either 1M ^{13}C formic acid (14.8mm OD), 1M [1-^{13}C]lactate (11.9mm OD), 1M [1-^{13}C]alanine (10.2mm OD) or 1M ^{13}C bicarbonate (19.6mm OD) to simulate the expected number of metabolites and chemical shift in a HP ^{13}C experiment. The RF pulse was centered on bicarbonate, and data were acquired with either a symmetric or flyback echo-planar trajectory, with a 1s TR, a FOV of 96 × 96mm, a matrix size of 32 × 32, and 60 averages, yielding a total 1 minute scan time. For the symmetric readout (**Fig. 1**) data were either fully encoded or acquired with a ramp-sampled, symmetric readout with partial Fourier reconstruction (75% k-space coverage in the k_y direction; **Table 1**). A reference scan was obtained directly on the ^{13}C channel by disabling the phase-encoding gradients and was acquired prior to imaging using 60 averages. Flyback EPI was reconstructed with a 2D Fourier Transform, while for ramp-sampled symmetric EPI the reference scan phase correction was applied (17), then data were interpolated to a Cartesian grid and 2D Fourier Transformed to image-space using the Orchestra reconstruction toolbox (GE Healthcare, WI, USA). The SNR was measured by calculating the mean signal within the phantom and then dividing by the standard deviation of the signal from a noise ROI. No changes to the Orchestra EPI routines were required for our ^{13}C EPI application, and the routines are fully automatic once the location of the reference scan and data are specified.

Unlike flyback EPI, symmetric EPI requires a reference scan to correct for timing delays and inconsistencies between even and odd lines of k-space. This can potentially be acquired on either the ^{1}H channel or directly on the ^{13}C channel.Due to the lack of endogenous ^{13}C, using the ^{13}C channel requires either an external ^{13}C enriched syringe or expending some hyperpolarized magnetization. To determine if a ^{1}H reference scan could provide a robust correction for ^{13}C images, reference scans were acquired on either the ^{1}H channel or on the ^{13}C channel from a natural abundance ethylene glycol phantom (outer diameter of 54mm, inner diameter of 24 mm) using the same trajectory (designed for a ^{13}C acquisition). The singleband SPSP pulse described above was used to avoid excitation of the J-coupled ^{13}C resonances. The matrix size and FOV were 32 × 32 and 72 × 72 mm, respectively, with partial Fourier (75% k-space coverage) in the phase-encode direction and ramp-sampling along the readout (0.492ms ramp duration, 0.380ms plateau duration, 1.364ms echo-spacing). A single 50 mm thick slice was excited, with 360 averages, a 0.5 s TR, and a 21.9 ms TE, with a total readout duration of 32.7 ms. Reference scans were applied to the ^{13}C data retroactively using the Orchestra Toolbox, and image quality was compared by calculating the fractional difference between the phantom data reconstructed with the two different reference scans.

To explore the utility of the ^{1}H reference scan for *in vivo* HP ^{13}C dynamic imaging, metabolites maps of pyruvate and lactate were acquired in the study of renal metabolism in a healthy rat. Metabolites were excited with a singleband SPSP RF pulse, with independent flip-angles designed to achieve the best estimates of perfusion and metabolic conversion rate parameters in a physiological model (18). A total of 25 timeframes for each metabolite were acquired over 50s, for a temporal resolution of 2s, with a FOV of 96 × 96mm and a matrix size of 32 × 32. Partial Fourier (75% k-space coverage) was used in the phase-encode direction along with ramp-sampling (0.452ms ramp duration, 0.240ms plateau duration, 1.144ms echo-spacing) to decrease the echo-time, yielding a TE of 20 ms with a 100ms TR per metabolite. Data acquisition started immediately prior to injection covering a 20mm axial slice centered on the kidneys. A reference scan was acquired on the ^{1}H channel using the ^{13}C trajectory prior to injection of the HP substrate. For comparison, a separate reference scan was directly acquired on the ^{13}C channel from the remaining hyperpolarized substrate magnetization following the final image. The efficacy of the ^{1}H reference scan was determined by calculating the structural similarity (SSIM) index (19) of [1-^{13}C]pyruvate for all time frames, and by comparing the time course between data reconstructed with either the ^{1}H or ^{13}C reference scan. For the SSIM index, the ^{13}C images reconstructed with the ^{13}C reference scan were considered the ground truth. SSIM is a measure of image quality and signal fidelity between two images, with an SSIM of 1 implying complete agreement between the two datasets. SSIM was chosen as the metric of comparison because it has been shown to be more sensitive to image shifts and overall changes in signal than mean square error (19,20).

Results

The results from the phantom study are shown in **Table 1** and **Supporting Figure 1**. The substantial SNR increase between flyback and symmetric EPI is due to the higher duty cycle for symmetric EPI, which encodes k-space on both the positive and negative readout lobes and reduces the TE. Further gains were observed when using ramp-sampling and a partial Fourier acquisition, as this further reduces the echo-time and increases the readout duty cycle, mitigating signal loss due to T_2* decay.

The ^{1}H reference scan provides a potential alternative method that is more robust and has higher SNR than direct acquisition on the ^{13}C channel. The reference scan in both cases was acquired using the ^{13}C trajectory, resulting in the same echo-spacing and timing delays for both approaches. The ^{13}C phantom images reconstructed without a reference scan show substantial ghosting (**Fig. 2A**). Qualitatively, the lack of Nyquist ghosting in the phantom images reconstructed with either the ^{1}H or ^{13}C reference scan (**Fig. 2B,C**) demonstrates the effectiveness of this technique. Quantitatively, the mean signal difference between both reconstruction approaches was <2% for all phantom voxels, further indicating that a ^{1}H reference scan was sufficient to correct for Nyquist ghosting in ^{13}C images.

This approach was further extended to the *in vivo* study of [1-^{13}C]pyruvate renal metabolism in a healthy rat. Images reconstructed with either a ^{13}C reference scan obtained from the residual hyperpolarization (**Fig. 3A**) or a ^{1}H reference scan obtained prior to ^{13}C imaging (**Fig. 3B**) are free of Nyquist ghosts. The SSIM index (**Fig. 3D**) was measured to be greater

than 0.91 for all timeframes using the ^{1}H reference scan, whereas the absence of a reference scan leads to Nyquist ghosting (**Fig. 3C**) and substantially lower structural similarity for all timeframes. The dynamic time course (**Fig. 3E**) was not significantly different (t-test, p = 0.98), further supporting the utility of a ^{1}H reference scan.

The *in vivo* dynamic data from a separate experiment can be seen in **Fig. 4**. Both pyruvate and lactate metabolite maps exhibit high SNR and are free of Nyquist ghost artifacts. The variable flip-angle schedule attempts to optimize the rate parameter estimates *in vivo*, yielding lactate images that provide nearly constant SNR throughout the time course. The absence of ghosting throughout the acquisition indicates that gradient heating and infidelity was not an issue, and a single reference scan was sufficient for phase correction for all time points. The higher spatial resolution of EPI (3mm in-plane) also enabled the visualization of differential metabolism between the renal cortex and medulla.

Discussion

In this study, we implemented and tested a ramp-sampled, symmetric, partial Fourier EPI sequence with spectral-spatial RF excitation for hyperpolarized ^{13}C imaging. The benefits of a symmetric readout were validated, and the feasibility of obtaining a suitable reference scan and artifact-free metabolite maps *in vivo* were demonstrated. In particular, ramp-sampling and partial Fourier further reduced the echo-spacing and TE for symmetric EPI, making it more robust to chemical shift artifacts in the slow phase encoding direction. In principle ramp-sampling and partial Fourier can result in an SNR penalty because of the reduction in total acquisition time and trajectory efficiency, but in practice this reduction is typically offset by the increase in SNR from the shorter TE and reduced echo-spacing. This acceleration will be crucial for the translation to clinical imaging, as the larger patient FOVs will necessitate a concomitant increase in matrix size to maintain adequate spatial resolution.

Estimating the timing delays between even and odd lines of k-space is crucial to minimizing ghosting artifacts in a symmetric EPI acquisition. We explored the reference scan correction using the ^{1}H channel, an external ^{13}C urea syringe, or the remaining magnetization from the hyperpolarized substrate. The external ^{13}C syringe works well for single, thick slice phantom studies but is problematic for thinner slices due to poor SNR or for multi-slice experiments when the imaging volume is larger than the phantom. While the reference scan using the residual hyperpolarization can also produce a suitable reference scan, it worked best in conjunction with a single-slice axial technique. This is an outcome of the experimental setup, since in-flowing spins provide fresh magnetization for a reference scan following a VFA scheme that ends at a 90-degree flip. For coronal slices, or for 3D imaging, this approach will likely prove difficult because of the lack of residual magnetization.

Instead, acquiring the reference scan from ^{1}H data is an appealing alternative. Complementary information from the ^{1}H channel has been previously shown to aid in ^{13}C reconstruction. For instance, a field map can be readily obtained on the ^{1}H channel and applied to ^{13}C data by accounting for the difference in gyromagnetic ratio (21), and the k-space trajectory can be measured using Duyn's method (22) on the ^{1}H channel and applied to ^{13}C data in a similar manner. Similarly, we have shown that a suitable reference scan can

be obtained in an analogous manner. This approach provided a more robust, higher SNR method to calculate the phase coefficients and correct for timing delays. The similarity in the computed coefficients, as well as the structural similarity index between images reconstructed with the ^{1}H or ^{13}C reference scan, implies that a ^{1}H reference scan can be acquired prior to and applied on hyperpolarized ^{13}C imaging to generate images that are free of Nyquist ghost artifacts. This technique is likely to be more robust than external ^{13}C syringes due to improved SNR and will be especially useful in clinical imaging where space considerations and patient comfort must be considered.

Other methods of accounting for timing delays in symmetric EPI have limitations. Doubly sampled EPI (23) can yield artifact free images by acquiring each line of k-space twice and separately reconstructing even and odd echoes. However this will substantially increase the echo-spacing and echo-time, resulting in signal loss and further filtering due to T_2* decay. Timing delays can also be estimated by acquiring two images, with the second shifted by one echo such that the even lines of k-space in the first image line up with the odd lines of k-space in the second image (24). This method effectively doubles the scan time and RF deposition, rendering it largely ineffective for hyperpolarized imaging. Navigator echoes are an alternative approach (25) that have also been shown to be effective in minimizing Nyquist ghosts. While it provides an updated reference scan for each timeframe, it does results in an increase in the TE. Calibrationless reconstruction techniques, such as minimizing the entropy in image-space (26), are an appealing alternative to a reference scan to mitigate Nyquist ghosting and will be explored in subsequent research.

Both spiral and Cartesian EPI are well-suited for single-shot imaging of hyperpolarized substrates, as both utilize high duty cycle and efficient trajectories (27-29). While a spiral acquisition has the benefit of a shorter echo-time and high SNR efficiency, it is more sensitive to off-resonance artifacts and gradient infidelities, but is robust to flow effects and pulsatile motion (30,31). Hyperpolarized pyruvate studies using spiral trajectories have relied on auto-focusing reconstruction methods to correct for off-resonance artifacts (8). EPI is more robust in the presence of off-resonance, resulting in either a benign shift in the PE direction for chemical shift or object distortion for an inhomogeneous B_0 field. Partial Fourier and parallel imaging techniques are also readily amenable to EPI trajectories and can be used to accelerate imaging (32), further reduce RF deposition, and reduce the TE for larger FOVs.

Conclusion

This ramp-sampled, symmetric EPI approach with spectral-spatial excitation of a single metabolite provided a fast, robust and clinically efficacious way to acquire hyperpolarized ^{13}C dynamic molecular imaging data. The substantial?SNR increase enables improved temporal and spatial localization and?increased scan coverage. The gains of this efficient sampling, combined with?partial Fourier methods, will be crucial for large matrix sizes required for?human-sized FOVs. This pulse sequence is well suited for clinical dynamic imaging of hyperpolarized substrates as it leverages well-established EPI methods to reconstruct ^{13}C metabolite maps on a commercial scanner in real time, and can be easily incorporated into existing diagnostic workflows.

Supplementary Material

Refer to Web version on PubMed Central for supplementary material.

Acknowledgements

We would like to thank Dr. Robert Bok for help with animal handling, Ralph Hurd and Wenwen Jiang for helpful discussions, and John Maidens for providing the dynamic flip angle designs.This work was supported by NIH grants R01 EB017449, R01 EB016741, and P41 EB013598.

References

1. Ardenkjær-Larsen JH, Fridlund B, Gram A, Hansson G, Hansson L, Lerche MH, Servin R, Thaning M, Golman K. Increase in signal-to-noise ratio of > 10,000 times in liquid-state NMR. Proc Natl Acad Sci USA. 2003; 100(18):10158–10163. [PubMed: 12930897]
2. Golman K, Olsson LE, Axelsson O, Mansson S, Karlsson M, Petersson JS. Molecular imaging using hyperpolarized 13C. Br J Radiol. 2003; 76(suppl_2):S118–127. [PubMed: 15572334]
3. Nelson SJ, Kurhanewicz J, Vigneron DB, Larson PEZ, Harzstark AL, Ferrone M, van Criekinge M, Chang JW, Bok R, Park I, Reed G, Carvajal L, Small EJ, Munster P, Weinberg VK, Ardenkjaer-Larsen JH, Chen AP, Hurd RE, Odegardstuen L-I, Robb FJ, Tropp J, Murray JA. Metabolic Imaging of Patients with Prostate Cancer Using Hyperpolarized [1-13C]Pyruvate. Science Translational Medicine. 2013; 5(198):198ra108.
4. Lupo JM, Chen AP, Zierhut ML, Bok RA, Cunningham CH, Kurhanewicz J, Vigneron DB, Nelson SJ. Analysis of hyperpolarized dynamic 13C lactate imaging in a transgenic mouse model of prostate cancer. Magnetic Resonance Imaging. 2010; 28(2):153–162. [PubMed: 19695815]
5. Reed GD, Larson PEZ, Morze Cv, Bok R, Lustig M, Kerr AB, Pauly JM, Kurhanewicz J, Vigneron DB. A method for simultaneous echo planar imaging of hyperpolarized 13C pyruvate and 13C lactate. Journal of Magnetic Resonance. 2012; 217(0):41–47. [PubMed: 22405760]
6. Cunningham CH, Chen AP, Lustig M, Hargreaves BA, Lupo J, Xu D, Kurhanewicz J, Hurd RE, Pauly JM, Nelson SJ, Vigneron DB. Pulse sequence for dynamic volumetric imaging of hyperpolarized metabolic products. Journal of Magnetic Resonance. 2008; 193(1):139–146. [PubMed: 18424203]
7. Cunningham CH, Chen AP, Albers MJ, Kurhanewicz J, Hurd RE, Yen Y-F, Pauly JM, Nelson SJ, Vigneron DB. Double spin-echo sequence for rapid spectroscopic imaging of hyperpolarized 13C. Journal of Magnetic Resonance. 2007; 187(2):357–362. [PubMed: 17562376]
8. Lau AZ, Chen AP, Ghugre NR, Ramanan V, Lam WW, Connelly KA, Wright GA, Cunningham CH. Rapid multislice imaging of hyperpolarized 13C pyruvate and bicarbonate in the heart. Magnetic Resonance in Medicine. 2010; 64(5):1323–1331. [PubMed: 20574989]
9. Du YP, Joe Zhou X, Bernstein MA. Correction of concomitant magnetic field-induced image artifacts in nonaxial echo-planar imaging. Magnetic Resonance in Medicine. 2002; 48(3):509–515. [PubMed: 12210916]
10. Le Bihan D, Poupon C, Amadon A, Lethimonnier F. Artifacts and pitfalls in diffusion MRI. Journal of Magnetic Resonance Imaging. 2006; 24(3):478–488. [PubMed: 16897692]
11. Bruder H, Fischer H, Reinfelder HE, Schmitt F. Image reconstruction for echo planar imaging with nonequidistant k-space sampling. Magnetic Resonance in Medicine. 1992; 23(2):311–323. [PubMed: 1549045]
12. Ahn CB, Kim JH, Cho ZH. High-Speed Spiral-Scan Echo Planar NMR Imaging-I. Medical Imaging, IEEE Transactions on. 1986; 5(1):2–7.
13. Derby K, Tropp J, Hawryszko C. Design and evaluation of a novel dual-tuned resonator for spectroscopic imaging. Journal of Magnetic Resonance (1969). 1990; 86(3):645–651.
14. Larson PEZ, Kerr AB, Chen AP, Lustig MS, Zierhut ML, Hu S, Cunningham CH, Pauly JM, Kurhanewicz J, Vigneron DB. Multiband excitation pulses for hyperpolarized 13C dynamic chemical-shift imaging. Journal of Magnetic Resonance. 2008; 194(1):121–127. [PubMed: 18619875]

15. Tsai C-M, Nishimura DG. Reduced aliasing artifacts using variable-density k-space sampling trajectories. Magnetic Resonance in Medicine. 2000; 43(3):452–458. [PubMed: 10725889]
16. Jiang W, Lustig M, Larson PEZ. Concentric rings K-space trajectory for hyperpolarized 13C MR spectroscopic imaging. Magnetic Resonance in Medicine. 2014 DOI: 10.1002/mrm.25577.
17. Hinks R, Mock B, Collick B, Frigo F, Shubhachint T. Method and system for image artifact reduction using nearest-neighbor phase correction for echo planar imaging. Google Patents. 2006
18. Maidens, J., Larson, PEZ., Arcak, M. Optimal Experiment Design for Physiological Parameter Estimation Using Hyperpolarized Carbon-13 Magnetic Resonance Imaging; Proceedings of the American Control Conference; Chicago, IL. 2015. FrC11.1
19. Zhou W, Bovik AC, Sheikh HR, Simoncelli EP. Image quality assessment: from error visibility to structural similarity. Image Processing, IEEE Transactions on. 2004; 13(4):600–612.
20. Zhou W, Bovik AC. Mean squared error: Love it or leave it? A new look at Signal Fidelity Measures. Signal Processing Magazine, IEEE. 2009; 26(1):98–117.
21. Gordon JW, Niles DJ, Fain SB, Johnson KM. Joint spatial-spectral reconstruction and k-t spirals for accelerated 2D spatial/1D spectral imaging of 13C dynamics. Magnetic Resonance in Medicine. 2014; 71(4):1435–1445. [PubMed: 23716402]
22. Duyn JH, Yang Y, Frank JA, van der Veen JW. Simple Correction Method for k-Space Trajectory Deviations in MRI. Journal of Magnetic Resonance. 1998; 132(1):150–153. [PubMed: 9615415]
23. Yang QX, Posse S, Le Bihan D, Smith MB. Double-sampled echo-planar imaging at 3 Tesla. Journal of Magnetic Resonance, Series B. 1996; 113(2):145–150. [PubMed: 8948138]
24. Hu X, Le TH. Artifact reduction in EPI with phase-encoded reference scan. Magnetic resonance in medicine. 1996; 36(1):166–171. [PubMed: 8795036]
25. Miller JJ, Lau AZ, Teh I, Schneider JE, Kinchesh P, Smart S, Ball V, Sibson NR, Tyler DJ. Robust and high resolution hyperpolarized metabolic imaging of the rat heart at 7 t with 3d spectral-spatial EPI. Magnetic Resonance in Medicine. 2015 DOI: 10.1002/mrm.25730.
26. Skare, S., Clayton, DB., Newbould, R., Moseley, M., Bammer, R. A fast and robust minimum entropy based non-interactive Nyquist ghost correction algorithm; Proceedings of the 14th Annual Meeting of ISMRM; Seattle, WA. 2006. Abstract 2349
27. Block KT, Frahm J. Spiral imaging: A critical appraisal. Journal of Magnetic Resonance Imaging. 2005; 21(6):657–668. [PubMed: 15906329]
28. Durst M, Koellisch U, Frank A, Rancan G, Gringeri CV, Karas V, Wiesinger F, Menzel MI, Schwaiger M, Haase A, Schulte RF. Comparison of acquisition schemes for hyperpolarised 13C imaging. NMR in Biomedicine 2015:n/a-n/a.
29. Tsao J. Ultrafast imaging: Principles, pitfalls, solutions, and applications. Journal of Magnetic Resonance Imaging. 2010; 32(2):252–266. [PubMed: 20677249]
30. Nishimura DG, Irarrazabal P, Meyer CH. A Velocity k-Space Analysis of Flow Effects in Echo-Planar and Spiral Imaging. Magnetic Resonance in Medicine. 1995; 33(4):549–556. [PubMed: 7776887]
31. Glover GH, Lee AT. Motion Artifacts in fMRI: Comparison of 2DFT with PR and Spiral Scan Methods. Magnetic Resonance in Medicine. 1995; 33(5):624–635. [PubMed: 7596266]
32. Arunachalam A, Whitt D, Fish K, Giaquinto R, Piel J, Watkins R, Hancu I. Accelerated spectroscopic imaging of hyperpolarized C-13 pyruvate using SENSE parallel imaging. NMR in Biomedicine. 2009; 22(8):867–873. [PubMed: 19489035]

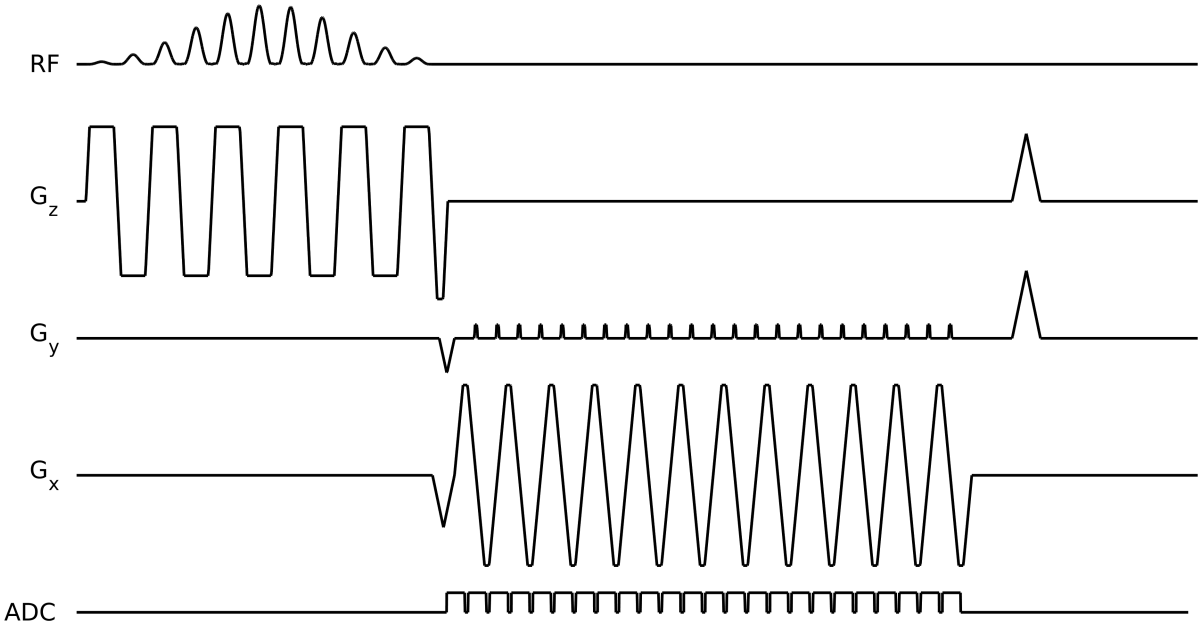

Figure 1.

Diagram of the symmetric EPI pulse sequence used in this work. The sequence consists of a singleband SPSP RF excitation, followed by a symmetric EPI readout. Phase errors due to timing delays are removed by a separate reference scan on the ^{1}H channel, accomplished by disabling the phase-encoding gradients.

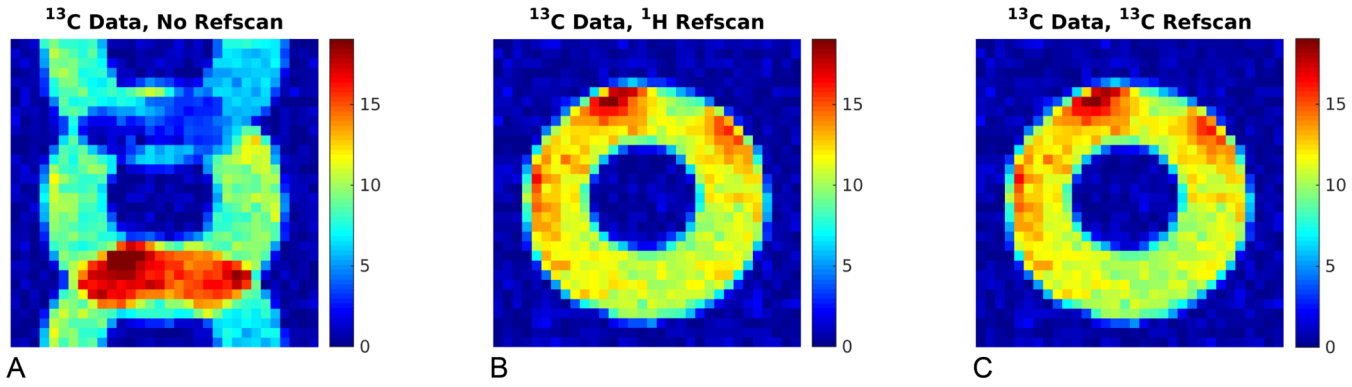

Figure 2.

The utility of a ^{1}H reference scan for ^{13}C EPI data. The uncorrected ^{13}C EPI image (A) exhibits strong Nyquist ghost artifacts in the absence of a reference scan. In contrast, ^{13}C phantom images reconstructed with either the ^{1}H (B) or ^{13}C (C) reference scan exhibit minimal ghosting, with a mean signal difference <2% between both reference scans for all phantom voxels. Using a ^{1}H reference scan is advantageous because it requires no external ^{13}C reference scan nor uses any hyperpolarized magnetization.

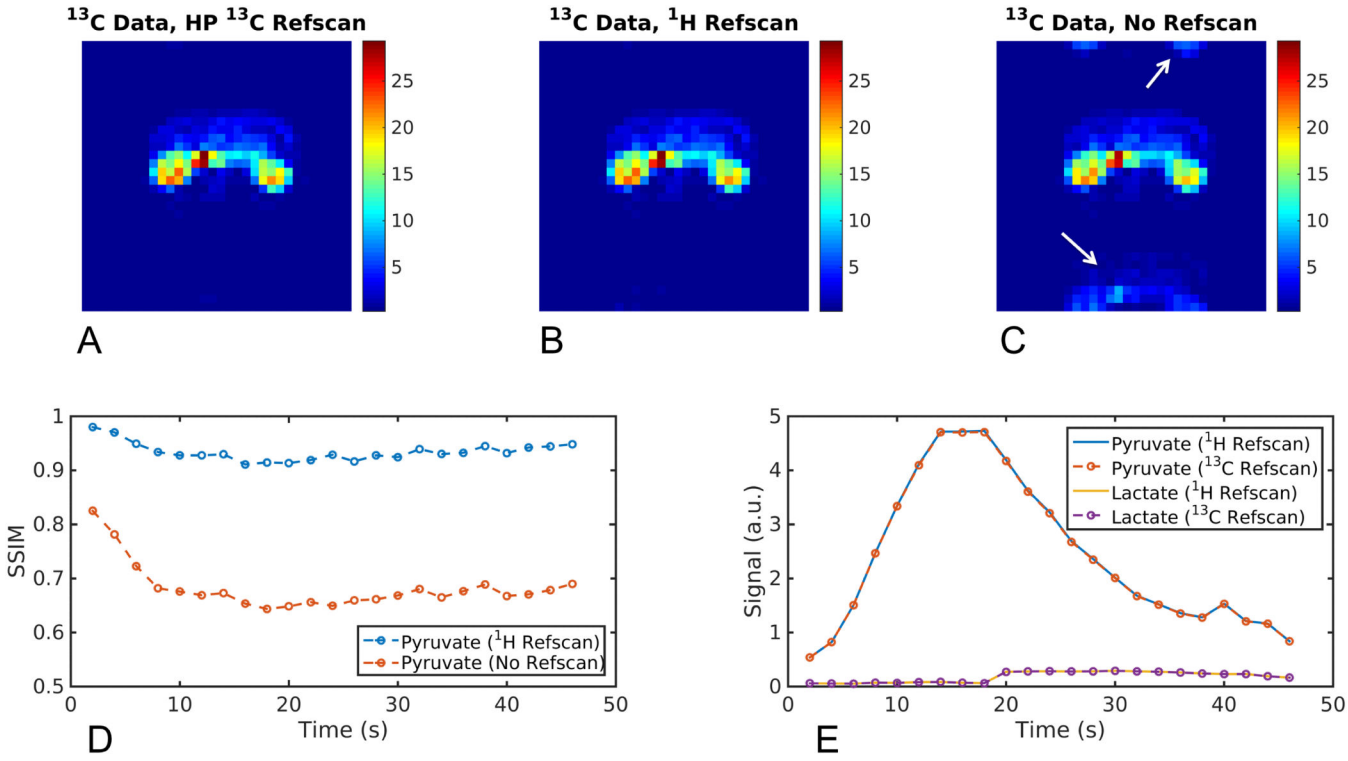

Figure 3.

In vivo validation of ^{1}H reference scan for ^{13}C EPI data. Representative images reconstructed with either the ^{13}C reference scan (A) or ^{1}H reference scan (B) are free of Nyquist ghosts, while the lack of a reference scan (C) clearly results in artifacts (arrows). The structural similarity index (SSIM; D) for pyruvate images reconstructed without a reference scan is substantially lower than data reconstructed using the ^{1}H reference scan. The ground truth was considered to be images reconstructed with the ^{13}C reference scan. The time course of pyruvate and lactate (E) is nearly identical for data reconstructed using either the ^{1}H or ^{13}C reference scan (< 0.5% difference).

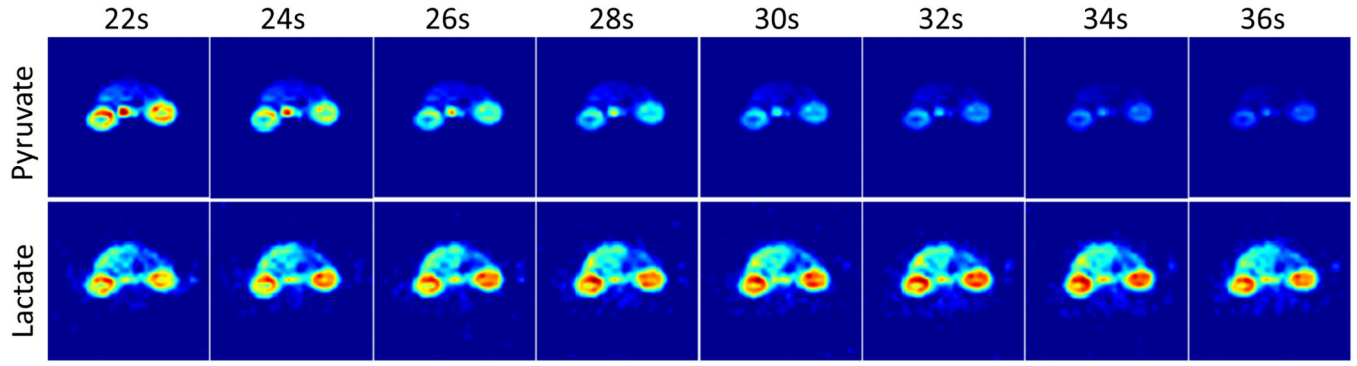

Figure 4.

Dynamic images of renal metabolism acquired with symmetric EPI. Both pyruvate and lactate metabolites images were free of Nyquist ghost artifacts and exhibit high SNR. Note the detail of differential metabolism between the renal cortex and medulla in the early pyruvate and lactate images that was enabled by the higher resolution EPI acquisition. Images have been zero-filled from 32×32 to 128×128 for display purposes.

Table 1

SNR and scan parameter comparison between EPI modes for a 96 x 96mm FOV and a 32 × 32 matrix. The improvement in measured SNR for the symmetric EPI modes is due to a higher duty cycle as well as shorter echo time.

	TE	Echo Spacing	Duty Cycle	Trajectory Efficiency	Relative SNR (Measured)
Flyback EPI	57.9 ms	2.24 ms	0.534	1.0	0.50 ± 0.03
Symmetric EPI	45.2 ms	1.74 ms	0.768	1.0	0.91 ± 0.07
Symmetric EPI with ramp sampling and partial-Fourier	26.4 ms	1.14 ms	0.92	0.879	1.0 ± 0.08